

Effect of Skin in Microwave Detection of Breast Cancer

ESKO ALANEN, STUDENT MEMBER, IEEE, AND ISMO V. LINDELL, SENIOR MEMBER, IEEE

Abstract—A calculation method is introduced and subsequent numerical results are shown for the effect of skin in radiometric detection of breast cancer using a horn antenna in direct contact with the skin. The electromagnetic problem in layered medium is solved applying the exact image theory, which enables the field calculation also in the near-field range. A proposal to optimize the aperture function for better resolution is given.

I. INTRODUCTION

MICROWAVE FREQUENCIES 2–6 GHz have proven to be useful in medical therapy and diagnostics. The penetration of energy in fat tissue is 3–5 cm. One of the serious difficulties is the poor resolution because the relevant distances are of the order of wavelength.

The illumination factor defined here as $\Delta T_a / \Delta T_t$, where ΔT_t is the temperature difference of fat and the tumor and ΔT_a is the temperature difference seen by the antenna, should be maximized. As pointed out in [1], the antenna response is determined by the near-field distribution. According to the reciprocity, it is obvious that this should decay rapidly from the maximum-field point.

Strict calculations of the field distribution in breast tissue can be made because it can be assumed that the fat layer is homogeneous. For the same reason, problems with microwave imaging are not present; rather, the difficulties originate from the noise radiation of fat tissue which should not cover the radiation from a cancerous growth. The skin can be also considered as a homogeneous layer and its effect can be calculated. It appears that it changes the phase and the absolute value of the electric-field components by only a small amount.

Previous approximative methods of field calculation in layered media based on the exact Sommerfeld formulation (e.g., the ray theory or the saddle point integration technique) are not valid at the distances of the order of wavelength. Therefore, the method presented in 1984 [2]–[4], known as the exact image theory, is applied in these calculations. The main advantage of the method is the fast convergence of the field integrals for all the locations of the field point, as shown in [2].

We consider a rectangular flanged horn antenna of a radiometer in direct contact with the skin. During some experimental research at Helsinki University of Technol-

ogy, the following questions have arisen: Should the aperture size be increased or decreased to get a greater concentration of the fields in the near-field range, and is there an aperture function, as has been proposed, e.g., in [5] and [6], which would offer better resolution at a certain depth than the ordinary ones? These earlier studies aimed towards a device for mass examination have motivated the present work.

The reciprocity is applied in the following calculations: the exact field components of a point source at the aperture plane are first presented. From these results, a proper phase variation for the aperture function is deduced. It is demonstrated that the area of the reciprocal focus can be reduced considerably in this way.

II. THEORETICAL MODEL

The construction of the theoretical model resulting in a three-layered symmetric problem is shown in Fig. 1(a)–(e). As an example, the following numerical values are assumed.

In Fig. 1(a), the horn antenna provided with a flange is placed on the skin of the thickness $d = 1.5$ mm. The relative dielectric factors of fat and skin are assumed to be $\epsilon_f / \epsilon_0 = 5.5 - j0.85$ and $\epsilon_s / \epsilon_0 = 44 - j14$, respectively, and the frequency is 5 GHz.

In Fig. 1(b), the Huygens' principle is applied: the whole body is surrounded with equivalent sources, whence the field outside the surface is zero.

In Fig. 1(c), the space left from the aperture level is filled with an ideal conductor and the tangential electric source can be omitted.

In Fig. 1(d), according to the image principle of an ideal conductor, the conducting material is replaced by an mirror image which doubles the magnetic source.

The problem in Fig. 1(d) is solved in the Fourier domain. The fields in region III can be expressed as the field arising from an image source in homogeneous fat tissue, as sketched in Fig. 1(e).

III. THE IMAGE SOURCES

The image sources in Fig. 1(e) can be derived by extending the formulation in [4] for the case in Fig. 1(d). The calculations are shown completely in [7] and partly in [8]. The main stages of these for a point-source $J_m = I_m L u_x \delta(\mathbf{r})$ are described as follows.

Manuscript received September 19, 1985; revised December 27, 1985. This work was supported in part by the Academy of Finland.

The authors are with the Department of Electrical Engineering, Helsinki University of Technology, Otakaari 5A, Espoo 15, Finland.

IEEE Log Number 8607624.

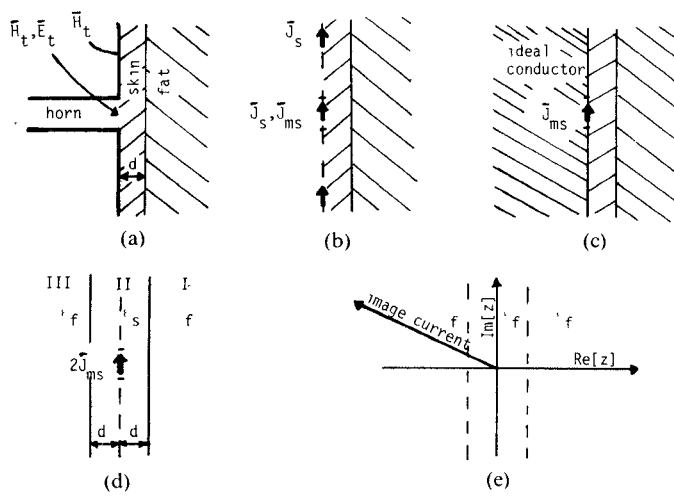


Fig. 1. Construction of the theoretical model.

The transmission-line analogy is exploited to solve the Fourier transform of the transverse electric field in region I of Fig. 1(d)

$$\mathbf{e}_1 = -I_m L [\mathbf{u}_y F(u) + \mathbf{K} (k_y/k^2) G(u)] \quad (1)$$

where

$$\mathbf{K} = k_x \mathbf{u}_x + k_y \mathbf{u}_y, \quad u = \sqrt{K^2 - \epsilon_f \mu \omega^2} \quad (2)$$

and where k_x and k_y are Fourier transform parameters. The inverse Laplace transforms of the functions $F(u)$ and $G(u)$

$$F(u) = \sum_i \int_{t_i} f_i(t_i) e^{-ut_i} dt_i \quad (3)$$

$$G(u) = \sum_j \int_{t_j} g_j(t_j) e^{-ut_j} dt_j \quad (4)$$

are substituted in (1). In (3) and (4), the path of each variable t_i or t_j are chosen separately on a complex plane.

Though the functions $F(u)$ and $G(u)$ are rather complicated, the transform functions $f_i(t_i)$ and $g_j(t_j)$ can be solved in a form of infinite exponential series due to the fact that $F(u)$ and $G(u)$ are single valued. Moreover, most of the exponential functions $f_i(t_i)$ and $g_j(t_j)$ are so rapidly decaying that they can be regarded as δ functions without any significant error.

The first term in (1) corresponds to a horizontal magnetic image and the second term a vertical electric image, respectively. The image sources in Fig. 1(e) for the point source can be finally expressed as follows:

$$\mathbf{J}_m(z') = -I_m L \delta(\mathbf{r}') \mathbf{u}_x F(0) \quad (6)$$

$$\mathbf{J}(z') = -j I_m L \frac{\epsilon_1}{Z_0} \frac{1}{k} \mathbf{u}_z \cdot \frac{\partial}{\partial y} [G_0 \delta(\mathbf{r}') + g_1 e^{u' t_1} \delta(\mathbf{r}')], \quad z' = -t_1 \quad (7)$$

where $u' = k(1.045 - j0.368)$ is the pole of $G(u)$ nearest to the origin, $g_1 = k(-0.297 + j0.103)$ is the corresponding residue, $G_0 = G(0) + g_1/u'$ and $\epsilon_1 = \epsilon_f/\epsilon_0$.

IV. ELECTRIC-FIELD COMPONENTS OF A POINT SOURCE

The effect of skin is demonstrated by comparing the fields of the horizontal dipole source $\mathbf{J}_m = I_m L \delta(\mathbf{r}) \mathbf{u}_x$ (without skin) and the sources (6), (7) (with skin) in homogeneous fat tissue. Special attention is paid here to the phase of the three components of the electric field because from this information a proper aperture function for the horn antenna can be deduced.

In Fig. 2, curves of the normalized absolute value and the phase of the field components E_y and E_z are shown at depths of $z = 1$ cm, 3 cm, and 5 cm. The curves are calculated along the lines $x = 0$, $y = 0 \dots 1.5$ cm and $y = 0$, $x = 0 \dots 1.5$ cm. With the skin effect, the curve along the line $x = 0$, $y = 0 \dots -1.5$ cm differs slightly from the curve $x = 0$, $y = 0 \dots 1.5$ cm; however, the difference is so small that the curves are not drawn separately. Solid lines are calculated with the skin effect while dotted lines correspond to the simple source without the skin effect.

It should be pointed out that E_x is zero along the above lines and E_z is zero along the line $y = 0$, $x = 0 \dots 1.5$ cm for both sources; for the magnetic current (6), this is obvious, and, for the electric current (7), this comes from the derivative operation $\partial/\partial y$.

V. APERTURE SYNTHESIS

In this section, we consider a rectangular horn antenna which is in direct contact with the skin. Several different aperture functions and sizes are introduced and for each the distribution of the field strength on the $z-x$ and $z-y$ planes are presented. It appears that by forcing the principal field component E_y to be summed coherently (equal phase of contributions from all points of the aperture) at the point $x = y = 0$, $z = 3$ cm, the hot spot reduces considerably if the aperture size is large enough.

The functions of the aperture shown in Fig. 3 are the following:

$$A(x', y') = \cos(x' \pi/a) \quad (8)$$

$$B(x', y') = Ap(x', y') \quad (9)$$

$$C(x', y') = \cos(x' \pi/a) - 0.5 \cos(3x' \pi a) \quad (10)$$

$$D(x', y') = Cq(x', y') \quad (11)$$

where $p(x', y')$ and $q(x', y')$ are phase functions with unit absolute values which equalize the phase of E_y at the point $x = y = 0$, $z = 3$ cm. The aperture sizes $a \times b$ are 3×2 cm 2 and 4×3 cm 2 . The absolute value of the electric field at the depths of $z = 1$, 3, and 5 cm are shown in Fig. 4. The solid lines correspond to the phase-corrected aperture, while the dotted lines are uncorrected, respectively. The Green's function used also included the near-field terms.

From the results in Fig. 4 can be seen that, for the smaller aperture, the phase correction does not significantly improve the field concentration. On the contrary, for the larger aperture, the difference is distinct. In fact, the focal extensions at $z = 3$ cm (focal area is defined here

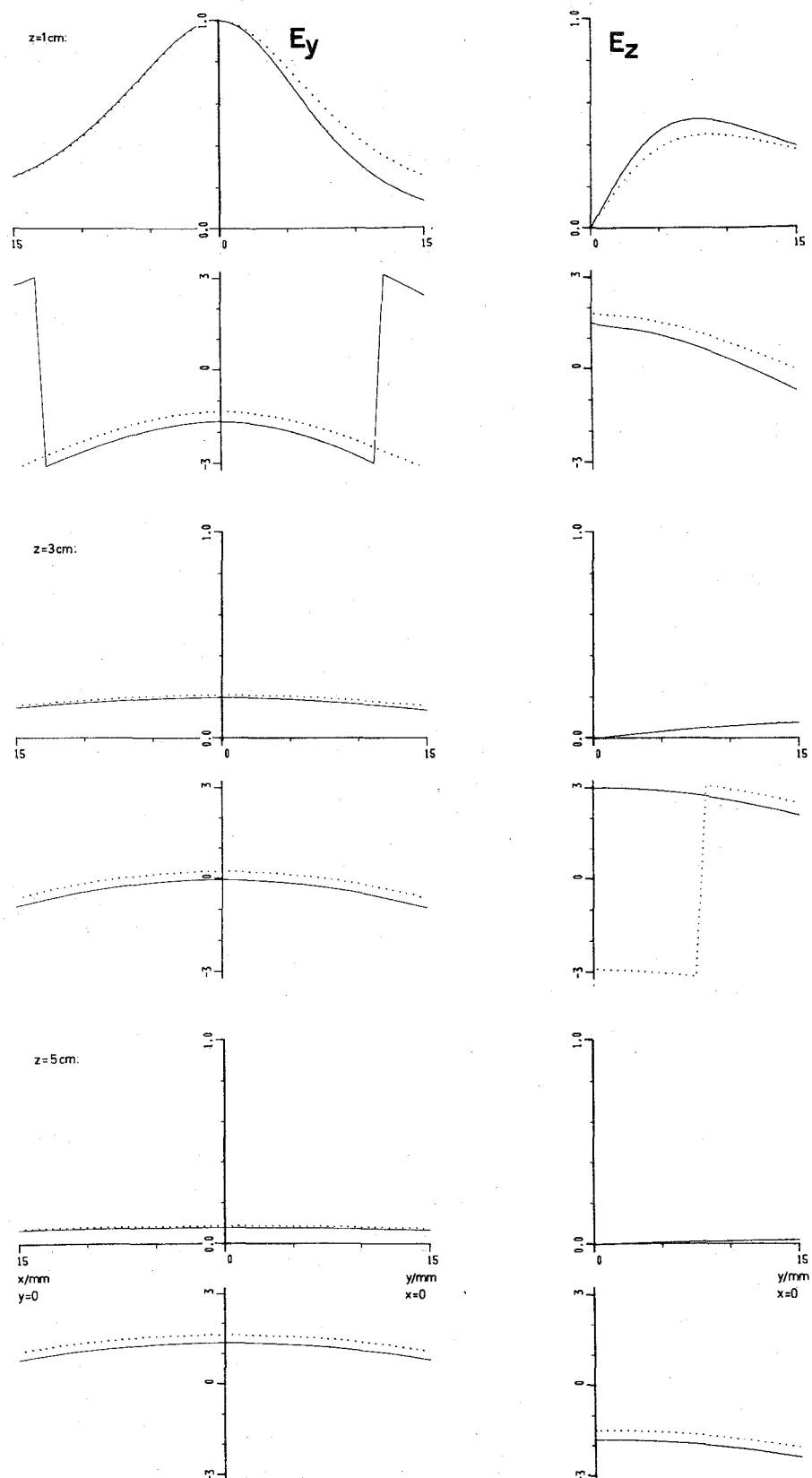


Fig. 2. Normalized absolute value and phase of the electric field components E_y and E_z at the depths 1, 3, and 5 cm for a point source with the effect of skin (solid lines) and without the effect of skin (dotted lines).

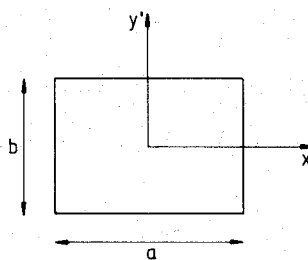


Fig. 3. Geometry of the aperture of the horn antenna.

TABLE I
FOCAL EXTENSIONS AT $z = 3$ cm FOR THE APERTURE $4 \times 3 \text{ cm}^2$

Function	A	B	C	D
$x_{3\text{dB}} / \text{mm}$	29	23	24	21
$y_{3\text{dB}} / \text{mm}$	42	28	41	24

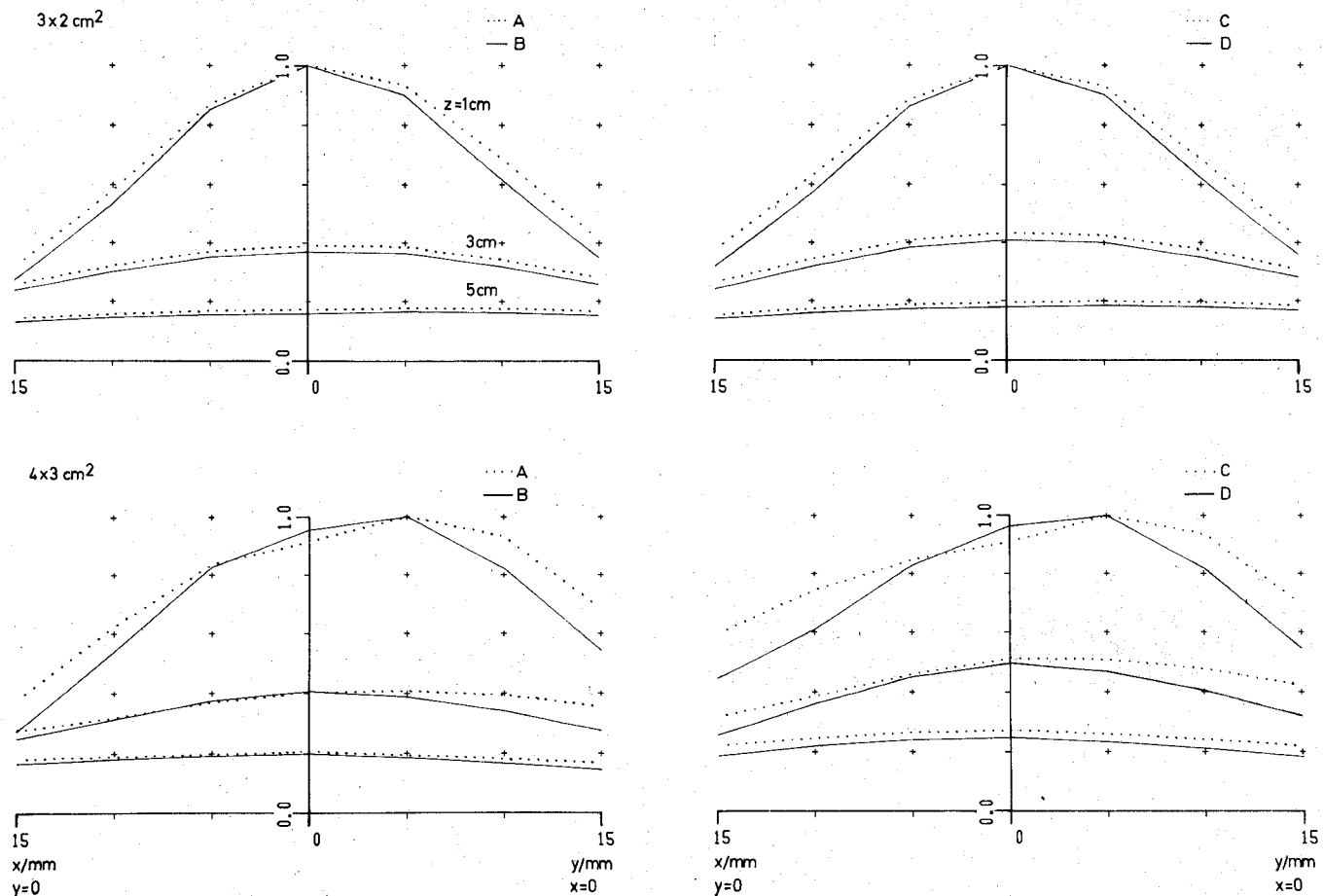


Fig. 4. Normalized distributions of the electric field for different aperture functions and sizes at the depths 1, 3, and 5 cm. Solid lines correspond to the phase-corrected aperture and dotted lines correspond to the constant phase apertures. Note that the energy distributions are proportional to the square of values above.

as the area surrounded by the 3-dB contour on a constant z -plane) along the lines $y = 0$ and $x = 0$ for the aperture size $4 \times 3 \text{ cm}$ and the four functions are shown in the Table I. The reduction of the field levels is also noticeable at a depth of 1 cm.

VI. CONCLUSION

With the present calculation method applying the exact image theory, a radiation problem in layered biological medium has been solved exactly. Human skin has been assumed to be a homogeneous layer and its effect has been demonstrated. It has been shown that by a proper phase variation of the aperture function of a horn antenna, the size of the hot spot can be reduced considerably in the case when the aperture is large enough.

REFERENCES

- [1] P. C. Myers, N. L. Sadowsky, and A. H. Barrett, "Microwave thermography: Principles, methods and clinical applications," *J. Microwave Power*, vol. 14, no. 2, pp. 105-115, June 1979.
- [2] I. V. Lindell and E. Alanen, "Exact image theory for the Sommerfeld half-space problem, Part I: Vertical magnetic dipole," *IEEE Trans. Antennas Propagat.*, vol. AP-32, pp. 126-133, Feb. 1984.
- [3] _____, "Exact image theory for the Sommerfeld half-space problem, Part II: Vertical electric dipole," *IEEE Trans. Antennas Propagat.*, vol. AP-32, pp. 841-847, Aug. 1984.
- [4] _____, "Exact image theory for the Sommerfeld half-space problem, Part III: General formulation," *IEEE Trans. Antennas Propagat.*, vol. AP-32, pp. 1027-1032, Oct. 1984.
- [5] P. S. Neelakantaswamy, K. K. Kupta, and D. K. Banerjee, "A Gaussian-beam launcher for microwave exposure studies," *IEEE Trans. Microwave Theory Tech.*, vol. MTT-25, pp. 426-428, May 1977.
- [6] Hao Ling and Shung-Wu Lee, "Focusing of electromagnetic waves through a dielectric interface," *J. Opt. Soc. Am. A*, vol. 1, no. 9, pp. 965-973, Sept. 1984.

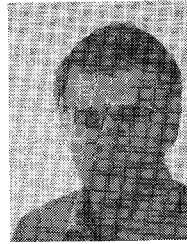
- [7] E. Alanen and I. V. Lindell, "Exact image method of field calculation for microwave radiation problems with layered biological media," Electromagnetics Laboratory, Helsinki University of Technology, Rep. 2, Apr. 1985.
- [8] ———, "Exact image theory for field calculation in layered biological medium," in *1985 Int. Microwave Symp. Dig.* (St. Louis), June 1985, pp. 78-81.

★



Esko Alanen (S'82) was born in Helsinki, Finland, on February 26, 1957. He received the degrees of Dipl. Eng. and Lic. Tech. in 1982 and 1986, respectively, in electrical engineering from the Helsinki University of Technology, Espoo, Finland.

He is working as a teaching assistant at the Electromagnetics Laboratory at the Helsinki University of Technology. His main interest is in electromagnetic theory.



Ismo V. Lindell (S'68-M'69-SM'83) was born in Viipuri, Finland, on November 23, 1939. He received the degrees of Dipl. Eng., Lic. Tech., and Dr. Tech. in 1963, 1967, and 1971, respectively, all in electrical engineering, from the Helsinki University of Technology, Espoo, Finland.

He was a Research and Teaching Assistant from 1963 to 1970, Acting Associate Professor or Acting Professor from 1970 to 1975 and 1984, and Associate Professor since 1975, in Radio

Engineering with the Helsinki University of Technology. During the academic year 1972-1973, he was a Visiting Associate Professor at the University of Illinois, Urbana. Since 1984, he has been Head of the Electromagnetics Laboratory. He is the Commission B Official Member of Finland in URSI and, since 1985, Chairman of the IEEE Finland Section, a TPC Member of the 1985 European Microwave Conference, and Member of the Editorial Board of the *Journal of Electromagnetic Waves and Applications*. He is the author of scientific papers and a book, *Radio Wave Propagation* (in Finnish). His main interest is in electromagnetic theory.